Excited states in ^{217}Ra populated in the α decay of ^{221}Th

E. Parr,[1,2] J. F. Smith,[1,2] P. T. Greenlees,[3] K. Auranen,[3] R. Chapman,[1,2] D. M. Cullen,[4] T. Grahn,[3] L. Grocutt,[1,2] A. Herzáň,[3,5] R.-D. Herzberg,[6] D. Hodge,[4] U. Jakobsson,[3,*] R. Julin,[3] S. Juutinen,[3] J. Konki,[3,†] C. McPeake,[6] D. Mengoni,[7] A. K. Mistry,[6] K. F. Mulholland,[1,2] G. G. O'Neill,[6] J. Pakarinen,[3] P. Papadakis,[3,‡] J. Partanen,[3] P. Peura,[3] P. Rahkila,[3] P. Ruotsalainen,[3] M. Sandzelius,[3] J. Sarén,[3] M. Scheck,[1,2] C. Scholey,[3] M. Siciliano,[3,7,§] M. Smolen,[1,2] J. Sorri,[3,‖] S. Stolze,[3,¶] M. J. Taylor,[4,#] and J. Uusitalo[3]

[1]*School of Computing, Engineering, and Physical Sciences, University of the West of Scotland, Paisley PA1 2BE, United Kingdom*

[2]*SUPA, Scottish Universities Physics Alliance, Glasgow G12 8QQ, United Kingdom*

[3]*University of Jyvaskyla, Department of Physics, P.O. Box 35, FIN-40014 University of Jyvaskyla, Finland*

[4]*Department of Physics and Astronomy, Schuster Building, The University of Manchester, Manchester M13 9PL, United Kingdom*

[5]*Institute of Physics, Slovak Academy of Sciences, SK-84511 Bratislava, Slovakia*

[6]*Oliver Lodge Laboratory, University of Liverpool, Liverpool L69 7ZE, United Kingdom*

[7]*Dipartimento di Fisica e Astronomia dell' Università and INFN Sezione di Padova, Padova, Italy*

(Received 5 June 2020; revised 30 September 2020; accepted 10 November 2020; published 30 November 2020)

Fine structure in the α decay of $^{221}_{90}$Th, populating excited states in $^{217}_{88}$Ra, was studied using $\alpha\gamma$-coincidence spectroscopy. Two α-decay branches from ^{221}Th have been newly observed, with E_α(keV)[b_α(%)] = 7951(8)[0.14(3)] and 8247(3)[1.51(12)], together with three previously known branches. Also, two new states in ^{217}Ra were identified at E = 177 and 227 keV. The ground-state configurations of the odd-A, N = 131 transitional isotones above ^{208}Pb are interpreted from their α-decay fine structure systematics and considered in terms of predictions using spherical shell and reflection-asymmetric models.

DOI: 10.1103/PhysRevC.102.054335

I. INTRODUCTION

Nuclei which reside between the closed shells at $Z = 82$, $N = 126$, and the region of strong octupole correlations in the light actinides [1–3] are often said to be shape *transitional*. The transition in shape is that between the spherical nuclear shapes at the shell closures, near ^{208}Pb, and the quadrupole and octupole deformed shapes in the light actinides, centered near ^{224}Ra. Transitional nuclei are of particular importance because small changes in nucleon numbers can cause dramatic changes in structure. Furthermore, these nuclei define the low-N boundary of the region of strong octupole correlations in the light actinides. In order to understand the structure of these nuclei, it is important to include not only single-particle excitations outside of the ^{208}Pb core, but also the effects of octupole correlations. For example, the structure of the states in the transitional radium nuclei around $A = 218$ can be explained using both the spherical shell model and the reflection-asymmetric model [4].

A useful experimental tool for studying low-lying excited states in nuclei is α decay. Low-spin states that are not populated in fusion-evaporation reactions may be populated following α decay. If the populated states in the daughter nucleus decay by γ-ray emission, then $\alpha\gamma$-coincidence measurements can give precise excitation energies. Hindrance factors (HFs) of the α decays also provide valuable information about the underlying structure of both the decaying and populated states. The HF value is defined as the ratio of the experimentally determined partial half-life of the α decay to the partial half-life calculated by a simple model where the preformed α particle lies in the potential of the daughter nucleus. Low HF values, close to unity, imply a similarity in structure between the initial and final states involved in the α decay, whereas high values imply a significant structural change. Thus the HF value could, for example, provide useful information in studying the decay from an octupole-deformed parent nucleus to a reflection-symmetric daughter nucleus.

The present work is concerned with the α decay of $^{221}_{90}$Th to the daughter nucleus $^{217}_{88}$Ra. The α decay of ^{221}Th has previously been studied in a number of experiments described in Refs. [5–10]. The α-particle energies, branching ratios, and half-lives published in those references are summarized in Table I. Three α-decay branches from the ground state of ^{221}Th have been consistently observed in the references, with α-particle energies of ≈8470, ≈8145, and ≈7730 keV.

*Present address: Department of Physics, KTH-Royal Institute of Technology, SE-10691 Stockholm, Sweden.

†Present address: CERN, CH-1211 Geneva 23, Switzerland.

‡Present address: Nuclear Physics Group, STFC Daresbury Laboratory, Daresbury, Warrington WA4 4AD, United Kingdom.

§Present address: IRFU, CEA/DSM, Université de Paris-Saclay, F-91191 Gif-sur-Yvette Cedex, France.

‖Present address: Radiation and Nuclear Safety Authority-STUK, Laippatie 4, Helsinki, Finland.

¶Present address: Physics Division, Argonne National Laboratory, Argonne, Illinois 60439, USA.

#Present address: Division of Cancer Sciences, School of Medical Sciences, The University of Manchester, Manchester M13 9PL, United Kingdom.

TABLE I. Details of the previously reported α-decay branches from the ground state of ^{221}Th. For each reference, the data given are the α-particle energies (E_α) in keV, together with the branching ratios (b_α) as a percentage, in square brackets. The half-life of the ground state of ^{221}Th ($T_{1/2}$) is given for several of the measurements, in units of ms.

Ref.	Valli *et al.* [5]	Torgerson and MacFarlane [6]	Andreyev *et al.* [7]
E_α (keV) [b_α]	7725(10) [6(1)%]	7733(8) [6%]	7730(10) [6%]
	8145(10) [56(3)%]	8146(5) [62.4%]	8150(10) [53%]
	8470(10) [39(2)%]	8472(5) [31.6%]	8265(10) [4%]
			8375(10) [11%]
			8470(10) [26%]
$t_{1/2}$ (ms)	1.8(3)	1.68(6)	1.7(3)
Ref.	Heßberger *et al.* [8]	Kuusiniemi *et al.* [9]	Liu *et al.* [10]
E_α (keV) [b_α]	7732(15) [4(3)%]	7732(4) [7%]	8134(45) [61(7)%]
	8135(10) [48(9)%]	8142(3) [72%]	8441(66) [39(6)%]
	8458(10) [48(9)%]	8469(4) [21%]	
$t_{1/2}$ (ms)	$2.0^{+0.3}_{-0.2}$	1.73(3)	

The lower-energy decays were shown to populate states with excitation energies ≈330 and ≈750 keV, while the higher-energy decay directly populates the ground state of ^{217}Ra. Two additional α-decay branches were reported in Ref. [7]. The measured half-life of the ^{221}Th ground state was reported to be ≈1.75 ms in the references listed above. In addition to α-decay spectroscopy, excited states in the daughter nucleus ^{217}Ra have been studied to high spin using in-beam γ-ray spectroscopy by Lönnroth *et al.* [11] and by Sugawara *et al.* [12], and using separate in-beam γ-ray and conversion-electron spectroscopy experiments by Roy *et al.* [13]. In these high-spin studies, the heavy-ion fusion-evaporation reactions ^{208}Pb(^{12}C, $3n$)^{217}Ra and ^{208}Pb(^{13}C, $4n$)^{217}Ra were used and over 20 excited states were identified up to spins of $J = 47/2\hbar$. However, there are some differences in the three level schemes constructed from these studies. In the present work, a total of five α-decay branches from the ^{221}Th ground state were observed, four of which populate excited states in the daughter nucleus ^{217}Ra. Two of the α-decay branches from ^{221}Th and two of the excited states in ^{217}Ra are observed for the first time.

II. EXPERIMENTAL DETAILS

The data presented here were obtained in an experiment that was performed at the Accelerator Laboratory of the University of Jyväskylä in Finland. The experiment was designed and optimized to study the excited states of ^{222}Th, produced in the ^{208}Pb(^{18}O, $4n$) reaction. The ^{221}Th nuclei, which are the subject of the present work, were produced as a subsidiary reaction product, via $5n$ evaporation. A beam of ^{18}O with energy 95 MeV and intensity ≈18 pnA was incident upon a self-supporting ^{208}Pb target of thickness 0.45 mg cm^{-2}, with a 0.1 mg cm^{-2} ^{12}C charge-reset foil downstream of the target. The beam was on target for approximately 157 h. The target was located at the center of the SAGE spectrometer [14], which was used to detect prompt γ rays and internal-conversion electrons; however, data from the SAGE spectrometer were not used for the α-decay studies in this work. Downstream of the target, recoiling evaporation residues were separated from fission fragments and unreacted beam ions using the RITU gas-filled recoil separator [15,16] and were transported to its focal plane.

At the focal plane of RITU the reaction products and their subsequent decays were further studied with a suite of detectors, including double-sided silicon-strip detectors (DSSDs), PIN-diode detectors, and Clover high-purity germanium (HPGe) detectors, which are part of the GREAT spectrometer [17]. The reaction products were implanted into the DSSDs placed side-by-side at the focal plane. Each DSSD had a thickness of 300 μm and consisted of 40 horizontal and 60 vertical strips giving a total of 4800 individual pixels. The 28 silicon PIN-diode detectors were arranged in a box array upstream of the DSSDs, and were used to detect charged particles which were emitted away from the DSSDs by the implanted nuclei. In normal operation, a multiwire proportional counter (MWPC) is placed upstream of the DSSD/PIN detectors. However, in the present experiment, the MWPC was not used due to the low energies of the evaporation residues. For the detection of x rays and γ rays emitted from implanted nuclei, three Clover HPGe detectors were placed around the DSSDs.

The analysis of data from the experiment was performed using the GRAIN software package [18], which was developed for use with data acquired by the Total Data Readout system [19].

III. DATA ANALYSIS

A. Calibrations and α-particle identification

The DSSDs were calibrated using the known energies of α particles emitted from evaporation residues, or their subsequent decay products, implanted into the DSSDs produced during the experiment. Specifically, the α decays used were from ^{210}Po [$E_\alpha = 5304.33(7)$ keV], ^{220}Ra [$E_\alpha = 7453(7)$ keV], ^{222}Th [$E_\alpha = 7603(3)$ and 7986(3) keV], ^{219}Ra [$E_\alpha = 7678(3)$ keV], and ^{213}Rn [$E_\alpha = 8088(8)$ keV]. Because the α-decaying nuclei were implanted into the silicon detector, a proportion of the energy of the recoiling daughter nucleus was also recorded and summed with that from the α particle

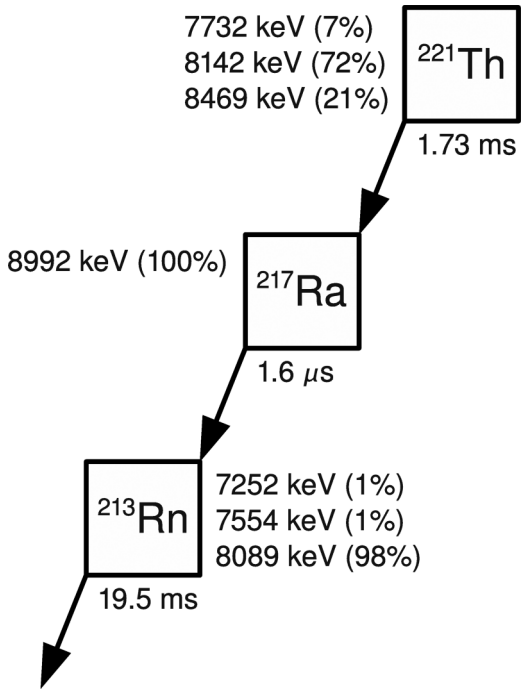

FIG. 1. α-decay chain of ^{221}Th-^{217}Ra-^{213}Rn-^{209}Po showing α-particle energies, branching ratios, and ground-state half lives, taken from Refs. [9,21,22].

[20]. The energies of the α particles used in the calibration, as well as those measured from ^{221}Th, were corrected for this effect.

The energy calibrations of the γ-ray detectors of GREAT were carried out using standard ^{152}Eu and ^{133}Ba calibration sources. The absolute efficiency for the detection of γ rays in the focal-plane Clover detectors as a function of γ-ray energy was determined by comparing the numbers of α particles in the DSSDs with numbers of $\alpha\gamma$ coincidences, where the multipolarities of the transitions were known and the intensities then corrected for internal conversion.

Figure 1 shows the ^{221}Th-^{217}Ra-^{213}Rn-^{209}Po α-decay chain, with data taken from Refs. [9,21,22]. The ^{221}Th α decays were identified in the analysis by selecting chains of either two or three signals within a single DSSD pixel. The first two signals corresponded to the implantation of a ^{221}Th recoil evaporation residue (an *implant*) followed by the α decay of the implant (a *decay*). The time difference between these first two signals was required to be between 0 and 12 ms, representing seven half-lives of ^{221}Th [$T_{1/2} = 1.73$ ms]. The third signal, where required, corresponded to the α decay of ^{213}Rn [$T_{1/2} = 19.5$ ms] and was required to be between 180 μs and 140 ms after the ^{221}Th α decay. The intervening α decay in the chain, ^{217}Ra, has a half-life of 1.6 μs and therefore due to the system dead time of around 6 μs was not used in the identification of ^{221}Th. The lower limit on the second time gate was imposed to prevent a large proportion of the abundantly produced ^{222}Th being included in the ^{221}Th spectra, the daughter of ^{222}Th, ^{218}Ra, having a half-life of 25.99(10) μs [23]. The requirement of the α decay from ^{213}Rn provided cleaner spectra, albeit with a reduction in statistics. The spectra presented here are from results requiring a second α decay, unless otherwise stated.

Normally, the GREAT spectrometer has an MWPC detector through which recoils must pass before being implanted into the DSSDs. Then, if a DSSD signal is preceded by an MWPC signal, the DSSD signal is assigned to be an implant; otherwise, it is assigned to be a decay. The MWPC was not used in the present experiment so an alternative method was employed: vetoing the assignment of signals as decays if a γ ray or internal-conversion electron was detected in the SAGE spectrometer at a time preceding the DSSD signal corresponding to the time-of-flight of recoils through RITU. In practice this requirement was made using a two-dimensional gate on a time-of-flight versus DSSD-energy matrix. The application of this veto reduced the number of signals from implanted nuclei included in the decay spectra.

B. α-particle conversion-electron energy summing

A complication of the experimental method used in this work is that the DSSD will not only detect the α particle emitted by the evaporation residue, but may also detect subsequent charged-particle emissions. This experimental phenomenon was previously addressed in Refs. [24,25]. In the present work, some of the α-decay branches populate excited states in the daughter nucleus, with the subsequent transitions proceeding by internal conversion, as well as γ-ray emission. This can lead to detector signal pile-up and a summed energy of the α particle and internal-conversion electron (α+ce) being recorded.

Consider a hypothetical decay scheme where α_1 populates a level in a daughter nucleus and α_2 a second level with energy E_γ greater than the first level. If the excited state populated by α_2 decays via internal conversion to the lower level then the α_2 and conversion electron may sum in energy. The difference in the energy measured between the summed α_2 and conversion electron with that of the α_1 is then given by $\Delta E = (E'_{\alpha 2} + E_{ce}) - E'_{\alpha 1}$, where E_{ce} is the energy of the conversion electron and E'_α is the total energy recorded following an α decay from a nucleus implanted into a detector. This total energy is the energy of the α particle plus a proportion of the recoiling energy of the daughter nucleus. This energy difference may also be approximated in terms of the difference in energy between the levels populated, E_γ, the atomic mass number of the α-decaying nucleus, A, the proportion of the recoiling daughter energy that is recorded in the detector, R, and the binding energy of the atomic electron ejected in the internal conversion process, BE, as

$$\Delta E \simeq E_\gamma \left[\frac{4}{A}(1-R)\right] - BE; \tag{1}$$

this formula is derived in the Appendix. A value of $R = 0.3$ has been used for any calculations, as this has been shown experimentally and theoretically to describe energy deposition from heavy nuclei [20,26]. The equation suggests that for certain α-decay level schemes the detected energy of a summed α particle from a decay to an excited state with an electron from an internally converted transition to a lower state may be identical to that of an α particle from a decay

which directly populates that lower state. This effect must therefore be considered when carrying out analysis of α-decay fine structure to avoid the misidentification as α decays of what are actually (α+ce) sums.

Although the (α+ce) summing effect is inconvenient when interpreting α-particle spectra, it may also be exploited to give an indication of the multipolarities of transitions. If the measured intensity of an α decay to an excited state is I_α and that of the α decay summed with an internal-conversion electron from any atomic shell emitted following the decay of the excited state is $I_{\alpha+ce(\text{total})}$, the total internal-conversion coefficient of the transition is given by

$$\alpha_{\text{total}} = \frac{I_{\alpha+ce(\text{total})}/\epsilon_e}{I_\alpha + I_{\alpha+ce(\text{total})} - (I_{\alpha+ce(\text{total})}/\epsilon_e)}, \qquad (2)$$

where ϵ_e is the efficiency for detecting an internal-conversion electron, where the branching ratio to the transition from the populated state is 100%. The value of ϵ_e may be found via geometric considerations of the current experimental setup. The transmission probability of 200-keV electrons, the maximum energy of conversion electrons presently considered in multipolarity calculations, through 300 μm of silicon, the DSSD thickness [17], is $\simeq$0% [27]. This, combined with the low implantation depth of the recoils in the DSSD detectors ($\approx$1.5 μs) [28], leads to an assumed efficiency of $\epsilon_e = 50\%$.

When using (α+ce) sum-peak intensities to measure internal-conversion coefficients from specific electron shells, Auger-electron yields must also be considered. In the case of high-energy Auger electrons, specifically those emitted when an electron vacancy in the K shell is filled, these can sum with K-shell conversion electrons to give similar energies to those expected following L- or M-shell conversions. However, as fluorescence yields following K-shell vacancies, ω_K, for heavy nuclei (with $Z \gtrsim 82$) are found to be $\omega_K \simeq 1$ [29], this effect may be ignored for the present results. The measured conversion coefficients from individual shells can therefore be found using the formula

$$\alpha_{K,L+M} = \frac{I_{\alpha+ce(K,L+M)}/\epsilon_e}{I_\alpha + I_{\alpha+ce(\text{total})} - (I_{\alpha+ce(\text{total})}/\epsilon_e)}, \qquad (3)$$

where $I_{\alpha+ce(K,L+M)}$ is the intensity of α decays summed with internal conversion electrons from the K or $L+M$ shells, conversion electrons from the latter two shells being measured as one intensity due to being unresolvable in silicon detectors.

Low-energy Auger electrons, emitted when electron vacancies in L and M shells are filled, can also sum with α-particle and (α+ce) energies. The energies of these Auger electrons are much lower than those emitted as a result of the filling of K-shell vacancies (up to $\approx$20 keV for radium). This means that their summing acts to broaden the width of α-particle and (α+ce) peaks, as opposed to introducing secondary peaks as discussed in Ref. [24]. These low-energy Auger electrons may be emitted following internal conversion of both L and M electrons as well as K electrons, the latter producing intermediate L- or M-shell vacancies following atomic electron reordering. The change in peak shape must therefore be considered when fitting (α+ce) intensities from K, as well as L and M, converted transitions; results from the present $\alpha\gamma$-coincidence study are shown in Fig. 2 to illustrate this effect. Both panels show the energies of α particles emitted in the decay to an excited state in the daughter nucleus. The top panel, however, shows the α-particle energies in coincidence with the γ ray which depopulates the excited state directly to the ground state, whereas the bottom panel shows those in coincidence with radium K x rays, ensuring the decay of the excited state populated in the daughter nucleus proceeds from the conversion of a K-shell electron. A clear broadening and shifting of the peak energy is observed from Auger-electron summing when the transition proceeds via K-shell conversion. This effect must be taken into account when measuring intensities of summed α-particle and conversion-electron intensities.

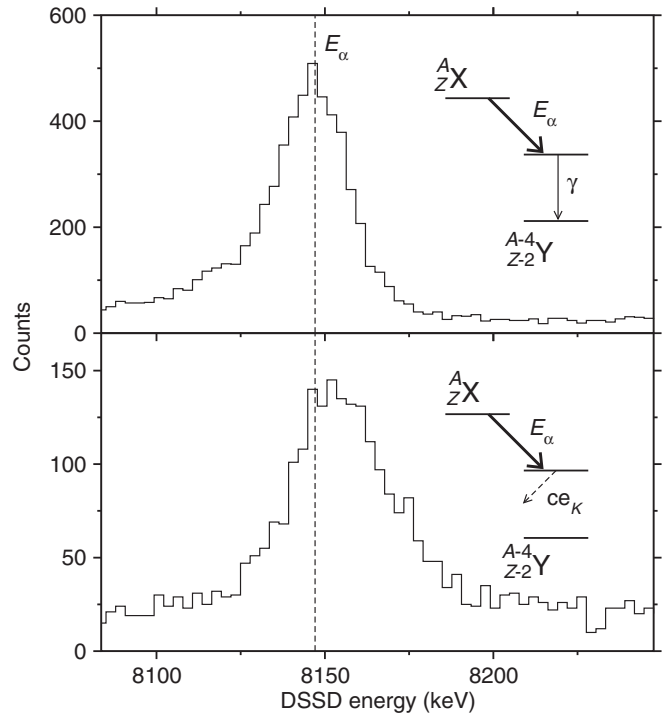

FIG. 2. α-particle energy spectra from $\alpha\gamma$-coincidence analysis. Upper and lower panels show energies in coincidence with 331-keV γ rays and K x rays from radium, respectively. Inset of each panel shows schematically the decay path which produces the spectra.

IV. RESULTS

Figure 3(a) shows the total DSSD spectrum taken over the course of the experiment. Figure 3(b) shows the spectrum of the first α decays in the selected implant-^{221}Th $\rightarrow$ (^{217}Ra) $\rightarrow$ ^{213}Rn $\rightarrow$ chains with the requirement of a ^{213}Rn α-particle energy (8088 keV) for the second decay. Due to the intermediate α decay of ^{217}Ra ($T_{1/2} = 1.6$ μs) low-energy distributions of summed energies between ^{221}Th α particles and those from the ^{217}Ra decay are observed, centered on energies around 100 keV above those of the ^{221}Th α particles. To remove these summed energy distributions the additional requirement of a signal in the PIN detectors between 1.5 and 10 μs after the ^{221}Th α-decay signal was implemented, with the resulting spectrum given in Fig. 3(c). Further details on the method

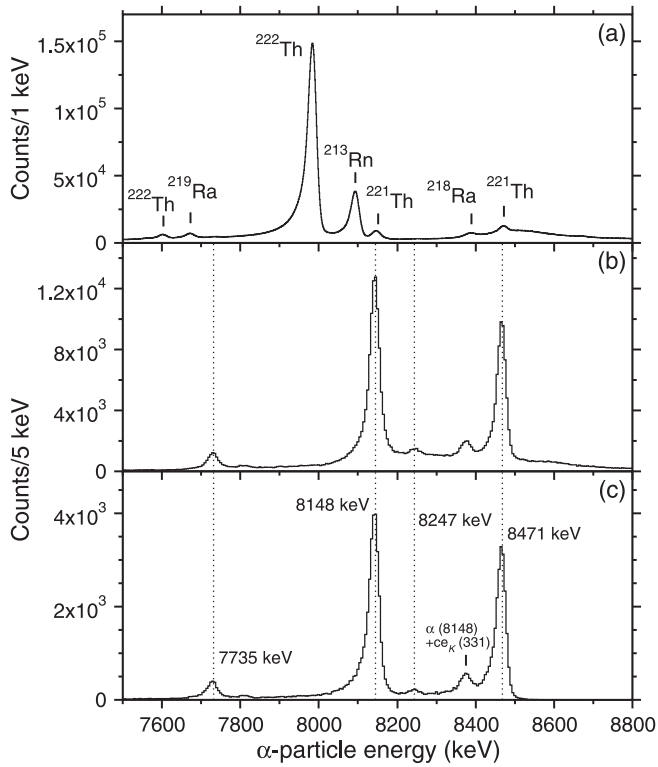

FIG. 3. (a) Total DSSD spectrum taken during the experiment. (b) DSSD spectrum of first α decay in implant-^{221}Th $\rightarrow$ (^{217}Ra) $\rightarrow$ ^{213}Rn correlated chains, with a ^{213}Rn α-particle energy also required. (c) Spectrum from (b) with the added requirement of a signal in the PIN detectors 1.5 μs after the first α decay. Energies from α decay of ^{221}Th that are visible in (c) are indicated and labeled.

of using PIN signals in delayed coincidence to obtain DSSD spectra without energy summing is given in Ref. [23].

In the study of α-decay fine structure, the sum of the Q value of the α decay from the ground state of the parent to an excited state in the daughter and the excitation energy of that state populated must be equal to the Q value of the ground-state-to-ground-state (parent-to-daughter) α decay. This fact can be useful in the identification of α-decay fine structure using $\alpha\gamma$ coincidences. In a two-dimensional spectrum of the energy recorded in the DSSD (equivalent to the α-decay Q value) versus the γ-ray energy, all of the $\alpha\gamma$ coincidences corresponding to decays between the same parent and daughter nuclei, which will populate excited states in the daughter nuclei that subsequently decay to the ground state via the emission of one γ ray, will lie on the same diagonal line. This line will intercept the DSSD energy axis at the value of the ground-state-to-ground-state parent-to-daughter α-decay Q value. Figure 4 shows spectra from the $\alpha\gamma$-coincidence analysis that was carried out in this work.

Figure 4(a) shows the ^{221}Th decays from the three-signal chains plotted against the energies of coincident γ or x rays. As no PIN signal in delayed coincidence was required, summed-energy signal distributions between ^{221}Th and ^{217}Ra α particles are present. The α particles from ^{221}Th can be identified with the aid of the dashed diagonal line shown in the spectrum of Fig. 4(a). This line represents a constant total Q value, Q_T, given as $Q_T = Q_\alpha + E_\gamma$, where Q_α is the α-particle Q value and E_γ is the γ-ray energy. Here the Q_T value is set to that of the ground-state-to-ground-state ^{221}Th $\rightarrow$ ^{217}Ra α decay, $Q_T = 8627$ keV. The $\alpha\gamma$ coincidences will lie on this line if the excited state populated in ^{217}Ra, following the α decay of ^{221}Th, subsequently decays via a γ-ray transition directly to the ground state. The figure reveals four α particles with γ-ray coincidences lying on the dashed line; they have energies of 7735, 7951, 8148, and 8247 keV. These α-particle energies are marked by horizontal dashed lines on Fig. 4(a) and are discussed individually below.

TABLE II. Details of the α decays from the ground state of ^{221}Th, measured in the present work. The values given are as follows: E_α is the energy of the α particle (in keV); b_α is the branching ratio (%); $J^\pi_{\rm pop}$ gives the spin and parity of the state in ^{217}Ra that is populated; $E_{\rm pop}$ is the excitation energy of the state populated in ^{217}Ra (in keV); Q_T is the total Q value of the α decay, given by $Q_\alpha + E_{\rm pop}$ (in keV); and HF is the hindrance factor for the decay.

E_α (keV)	b_α (%)	$J^\pi_{\rm pop}$	$E_{\rm pop}$ (keV)	Q_T	HF
7735(3)	4.7(2)	$(7/2)^+$	753	8630(3)	2.7(2)
7951(8)	0.14(3)	$13/2^+$	540	8637(8)	410(90)
8148(3)	60.3(7)	$11/2^+$	331	8629(3)	3.9(2)
8247(3)	1.51(10)	$(7/2,9/2)^-$	227	8626(3)	306(20)
8471(3)	33.4(4)	$9/2^+$	0	8627(3)	58(2)

A. ^{221}Th $\rightarrow$ ^{217}Ra α decays

In total, five α decays have been observed from ^{221}Th in this work. Properties of the α decays are given in Table II, including the energies, total Q_T values, branching ratios, and hindrance factors. Calculation of the hindrance factors required experimental and theoretical half-lives of ^{221}Th. The theoretical half-lives were calculated using the method described by Preston [30]. The experimental half-life was measured in this work to be 1.73(2) ms. This value is consistent with each of those previously reported, which are given in Table I.

The low uncertainty on the half-life measured in the present work is due to several factors: (i) the high yield of ^{221}Th nuclei produced, (ii) the recoil-mother-daughter analysis used to cleanly identify the ^{221}Th nuclei (described in Sec. III A), and (iii) the high pixelation of the DSSDs, which led to an average recoil implantation rate of around one implant every 40 s in each pixel. This low recoil-implantation rate meant that the rate of randomly correlated recoils and ^{221}Th α decays was negligible when combined with the short half-life of ^{221}Th.

1. E_α = 7735, 8148, 8471 keV

α particles with energy 8471 keV were identified using the α-particle spectra alone. These α particles are not prominent in Fig. 4(a) because they were only in coincidence with background γ rays. The high energy of this α decay relative to the others observed and the lack of $\alpha\gamma$ coincidences suggest that this α decay populates the ground state of ^{217}Ra. Coin-

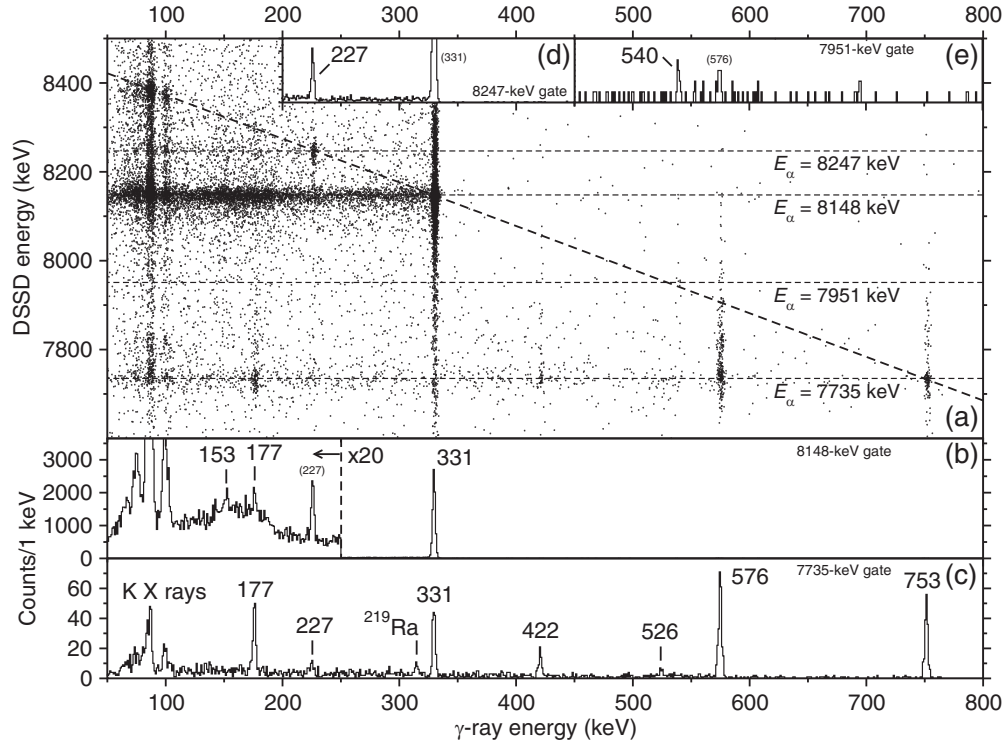

FIG. 4. Spectra from the $\alpha\gamma$-coincidence analysis in the decay of ^{221}Th. (a) The energy recorded in the DSSD versus the γ-ray energy (from the focal-plane Clover HPGe detectors). The energies of the four α particles from the decays to excited states in ^{217}Ra are shown as horizontal dashed lines. The diagonal dashed line indicates a constant Q_T value (Q_α+E_γ), set as the energy difference between the ground states of ^{221}Th and ^{217}Ra, 8627 keV. Shown are the γ-ray spectra in coincidence with the (b) 8148-keV (or that summed with a conversion electron from either of the 153- or 177-keV transitions), (c) 7735-keV, (d) 8247-keV, and (e) 7951-keV α particles.

cidences between α particles with energies 8148 and 7735 keV and γ rays of 331 and 753 keV, respectively, can be seen in Fig. 4(a), with the corresponding coincident γ-ray spectra shown in Figs. 4(b) and 4(c). As these coincidences lie on the ground-state-to-ground-state Q-value line (dashed diagonal), it is suggested that the α decays populate states with energies equal to those of the coincident γ rays. This is also supported by the measured Q_T values for the α decays in Table II.

2. E_α = 8247 keV

Coincidences between 8247-keV energy signals in the DSSDs and 227-keV γ rays are observed in Fig. 4(a), with the projected γ-ray coincidences shown in Fig. 4(d). These coincidences lie on the ground-state-to-ground-state Q-value line and therefore have a Q_T value consistent with the other α decays identified. There are two possible origins for these coincidences. The first possibility is that a single α decay with $E_\alpha = 8247$ keV directly populates a state with 227-keV excitation energy. The second possibility is that of an (α+ce) summing instance where an α decay with an α-particle energy less than 8247 keV (in this case likely to be the 8148-keV α particle) populates a higher-lying excited state and the α-particle energy sums with the L or M internal-conversion electron from the decay of that state to the 227-keV level. In this case the ΔE values from Eq. (1) would be -16 keV (α+ce$_L$) and -3 keV (α+ce$_M$). Here, the observed coincidences are thought to be due to 8247-keV α particles from decays to a state with excitation energy of 227 keV, for the reasons discussed below. In the case of (α+ce) summing, the energy of the transition which proceeds by internal conversion would be 104 keV. The γ rays in coincidence with the 8148-keV α particle are shown in Fig. 4(b), but there are no γ rays observed at 104 keV. Also, given that 50% of conversion electrons will not be detected, in the (α+ce) case, at least as many 227-keV γ rays would be expected to be observed in coincidence with the 8148-keV α particles as with the energy sum around 8247 keV. These coincidences are not observed. For these reasons, it is assumed that the 8247-keV peak in the DSSD spectrum is not due to (α+ce) summing, and it is assigned as an 8247-keV α particle, populating a state with excitation energy 227 keV.

3. E_α = 7951 keV

Coincidences between 7951-keV energy signals in the DSSD and 540-keV γ rays are shown in Figs. 4(a) and 4(e), the spectrum in Fig. 4(e) being taken using implant-^{221}Th chains, where no second α-decay identification was required. As these coincidences lie on the ground-state-to-ground-state Q-value line and have a consistent Q_T value with the other α decays they again have two possible origins. Either an α decay with an associated $E_\alpha = 7951$ keV populates an excited state at 540 keV, or the α decay with $E_\alpha = 7735$ keV to the 753-keV state is followed by an unobserved 213-keV transition to the 540-keV state, which then decays by a 540-keV γ-ray

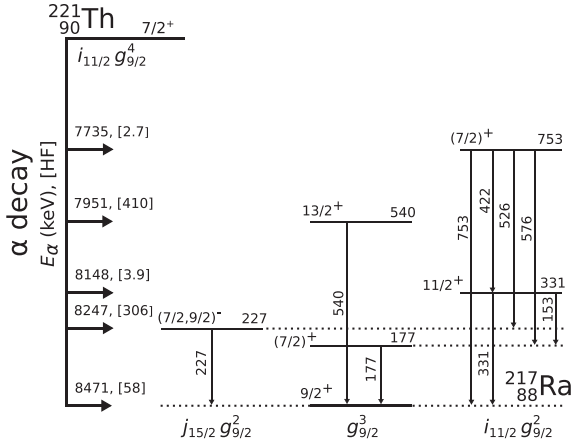

FIG. 5. Level scheme showing the excited states of ^{217}Ra populated following the α decay of ^{221}Th, deduced in this work. The left-hand side of the figure shows the α-decay transitions together with their energies and hindrance factors. The assigned spherical shell-model configurations are given below the levels.

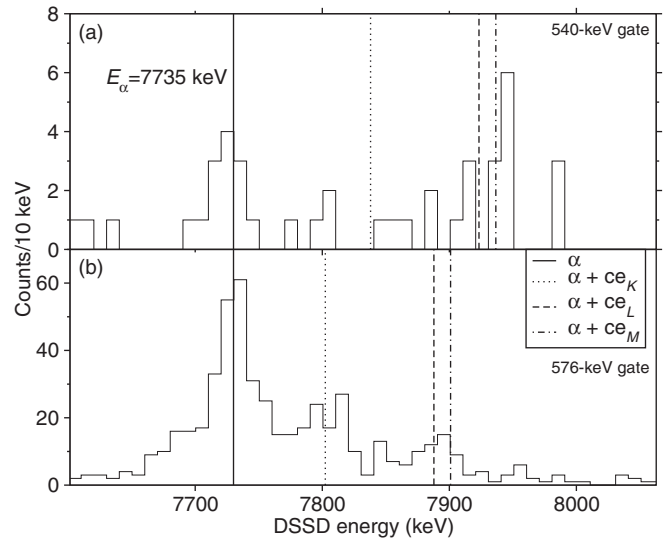

FIG. 6. DSSD energy spectra in coincidence with the (a) 540- and (b) 576-keV γ rays. The energy of the 7735-keV α particle is indicated by the solid vertical line. The dotted, dashed, and dot-dashed lines show the expected α+ce sum energies with K, L, and M internal-conversion electrons, respectively, from a (a) 213-keV and (b) 177-keV transition.

transition. Here the ΔE values would be -15 keV (α+ce$_L$) and -1 keV (α+ce$_M$).

The excited states of ^{217}Ra are discussed in the following section and are shown in Fig. 5. Considering an α+ce summing origin for the ($\alpha\gamma$) coincidences the hypothetical 213-keV transition would have an $M3$ multipolarity. As this transition would be unlikely to compete with those of higher-energy and lower-order multipolarities observed from the 753-keV state, this scenario is ruled out. However, due to uncertainty of the spin assignment for the 753-keV state, the possibility of lower-order multipolarities for the possible 213-keV transition will also be considered.

Figure 6(a) shows the DSSD spectrum in coincidence with the 540-keV γ ray. The relative intensities of these peaks can shed light on the possible (α+ce) summing issue. In the spectrum, the energy of the 7735-keV α particle is marked by a solid vertical line and the energies of the 7735-keV α particle summed with the K, L, and M internal-conversion electrons from a 213-keV transition are shown by the dotted, dashed, and dot-dashed vertical lines, respectively.

Considering an $E2$ multipolarity assignment for the 213-keV transition a conversion coefficient of $\alpha_{L+M} = 0.30$ would be expected [31]. This leads to the expectation that approximately seven times more 7735-keV α particles would be seen in coincidence with the 540-keV γ rays as those summed with the L or M conversion electrons from a 213-keV transition, when taking into account the 50% conversion-electrons detection efficiency. As this is not observed, along with the absence of the 213-keV γ ray in coincidence with the 7735-keV α particle in Fig. 4(c), the possibility of an $E2$ 213-keV transition is ruled out. Considering an $M1$ assignment for the 213-keV transition would give a conversion-coefficient ratio of $\alpha_K/\alpha_{L+M} = 4.38$. This would lead to the same ratio in intensities for the (α+ce) summed peaks from the K and L or M conversion electrons in Fig. 6(a). As this is also not the case, an $M1$ 213-keV transition can also be ruled out. For these reasons it is deemed that the coincidences between 7951-keV DSSD energy signals and 540-keV γ rays are due to a newly observed decay with α-particle energy 7951 keV directly populating a 540-keV state. It should be noted that the 7735-keV α-particle energies seen in coincidence with 540-keV γ rays in Fig. 6(a) are attributed to Compton scattering from the intensely produced 753- and 576-keV γ rays. Figure 6(b) is discussed in Sec. IV C.

B. ^{217}Ra level scheme

The proposed level scheme of excited states in ^{217}Ra populated by the α decay of ^{221}Th is shown in Fig. 5. The properties of the γ rays that have been observed in coincidence with ^{221}Th α particles are listed in Table III. The starting point in the construction of the level scheme was the inclusion of the four excited states that are directly populated by α decays from ^{221}Th, identified in Sec. IV A. Figure 4(c) shows a number of γ rays in coincidence with 7735-keV α particles, where the γ ray with energy 753 keV directly populates the ^{217}Ra ground state. The pairs of γ rays with energies of 331 and 422 keV, 227 and 526 keV, and 177 and 576 keV all sum to 753 keV so they have been assigned as three cascades, each of two transitions, from the 753-keV state to the ground state. The ordering of transitions in the first two cascades is defined by the previously established states at 331 and 227 keV. No α decay has been identified to a state which has the energy of either of the γ rays in the 177- and 576-keV cascade, leaving the ordering ambiguous. However, a cascade of 153- and 177-keV transitions from the 331-keV state may be established from the γ-ray spectrum shown in Fig. 4(b). The γ-ray spectrum was taken in coincidence with 8148-keV α particles, or these α-particle energies summed with conversion-electron energies emitted from the highly converted 153- and 177-keV

TABLE III. Properties of γ-ray transitions emitted from states in ^{217}Ra, following the α decay of ^{221}Th, as measured in this work. The column labeled E_γ gives the energy of the γ ray (in keV). The column labeled "Mult." gives the assigned multipolarity of the transition, as discussed in the text. The columns labeled J_i^π and J_f^π give the assigned spins and parities of the initial and final states and that labeled $I_{\rm rel}$ gives the relative intensities of the γ rays, corrected for detection efficiency. The column labeled E_α gives the energy of the α particle of the decay which precedes the γ ray for which the intensity was taken.

E_γ (keV)	Mult.	J_i^π	J_f^π	$I_{\rm rel}$	E_α (keV)
153.1(4)	$E2$	$11/2^+$	$(7/2)^+$	9(2)	8148
177.0(2)	$M1$	$(7/2)^+$	$9/2^+$	27(2)	7735
177.0(2)				12(2)	8148
226.7(2)	$E1$	$(7/2,9/2)^-$	$9/2^+$	6(2)	7735
226.7(2)				29(2)	8247
330.7(2)	$M1/E2$	$11/2^+$	$9/2^+$	8(2)	7735
330.7(2)				1000(10)	8148
421.8(2)	$E2$	$(7/2)^+$	$11/2^+$	14.1(14)	7735
525.8(3)	$E1$	$(7/2)^+$	$(7/2,9/2)^-$	3.6(9)	7735
539.8(3)	$E2$	$13/2^+$	$9/2^+$	2.3(6)	7951
575.6(2)	$M1$	$(7/2)^+$	$(7/2)^+$	77(3)	7735
752.6(2)	$M1$	$(7/2)^+$	$9/2^+$	43(3)	7735

transitions. This is the reason the 227-keV γ ray is also observed. This defines the 177-keV transition as the lower in the 177- and 576-keV cascade, and also therefore in the 153- and 177-keV cascade; a state at 177 keV is also then defined.

Despite the low numbers of counts in the spectra, an attempt has been made to test the proposed level scheme using $\gamma\gamma$-coincidence analysis. Figure 7 shows individual $\gamma\gamma$-coincidence spectra gated on seven γ-ray energies, which depopulate the 753-keV state. The gating transitions are indicated on each of the panels on the spectra. The results were obtained by gating on implant-^{221}Th chains. The coincidence spectra generally support the proposed level scheme. It should perhaps be noted that coincidences are not observed between

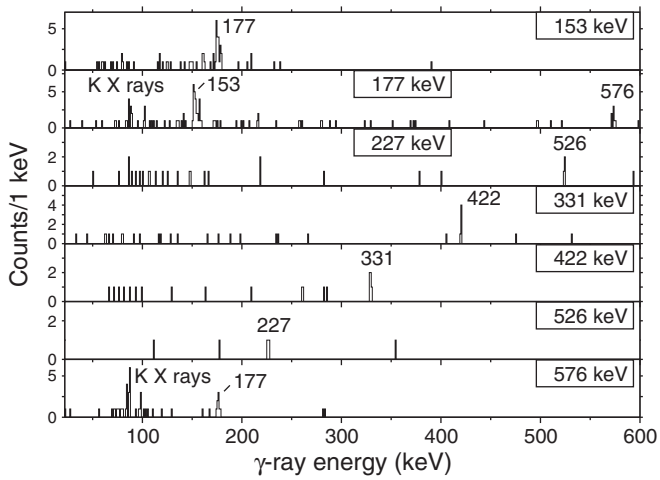

FIG. 7. $\gamma\gamma$-coincidence spectra, following the α decay of ^{221}Th. The energy of the γ-ray gate is indicated on each panel.

the 422-keV γ ray and either of the 153- or 177-keV γ rays. This is presumed to be due to the much lower α-decay branching ratio to the 753-keV state compared with that to the 331-keV state.

C. J^π of levels and multipolarities of transitions in ^{217}Ra

The spins and parities assigned to the observed states are given on the level scheme in Fig. 5 and the assigned multipolarities of transitions are listed in Table III. The spin and parity of the ground state of ^{217}Ra were previously assigned as $J^\pi = 9/2^+$ [11–13]. This assignment was made by shell-model considerations, where the three neutrons above the $N = 126$ closed shell have the configuration $\nu(g_{9/2})^3$. An unhindered (HF = 2.3) [5] α decay from ^{217}Ra to the ground state of ^{213}Rn agrees with the $9/2^+$ assignment. The spin and parity of the ^{221}Th ground state is assigned as $7/2^+$. This is based on theoretical and systematics arguments, presented in Ref. [32], which provide strong evidence for this assignment.

The 331- and 540-keV γ rays were observed in the work of Refs. [12,13], where the multipolarities of these transitions were determined to be $M1/E2$ and $E2$, respectively, using γ-ray angular-distribution measurements and internal-conversion coefficients. The spins and parities of the states at 331 and 540 keV were assigned as $11/2^+$ and $13/2^+$, respectively.

For the 177- and 153-keV γ-ray transitions, the (α+ce) summed intensities can be used to help determine the internal-conversion coefficients, from which the multipolarities can be inferred. This method was described in Sec. III B. Figure 6(b) shows the DSSD energies in coincidence with the 576-keV γ rays, ensuring only the α decays with $E_\alpha = 7735$ keV which subsequently decay via the 177- and 576-keV cascade contribute to the intensities. The energies of the 7735-keV α particle, along with those of the α-particle energy summed with the K, L, and M internal-conversion electrons from the 177-keV transition are indicated by the vertical lines. The total internal-conversion coefficients were determined using Eqs. (2) and (3). These conversion coefficients are given in Table IV along with the calculated values for different multipolarities [31]. This analysis suggests that the 177-keV transition has $M1$ character. It should be noted that a mixed $M1 + E2$ 177-keV transition with mixing ratio $\delta = 0.5$ would optimize the fit of the calculated conversion coefficients with the values determined experimentally [31]. However, due to the large uncertainties of the experimental conversion coefficients a pure $M1$ transition is assigned. This leads to possible assignments of $J^\pi = (7/2, 9/2, 11/2)^+$ for the 177-keV state.

To determine the internal-conversion coefficient of the 153-keV transition, a comparison of the intensities of the 177-keV γ ray in coincidence with the 8148-keV α particle and also with the 8148-keV α particle summed with internal-conversion electrons from the 153-keV transition can be used. As no 177-keV γ rays were observed in coincidence with the α particle summed with the K-shell conversion-electron energy from the 153-keV transition, an upper limit was found for α_K. The results of this analysis, given in Table IV, suggest an $E2$ assignment for the 153-keV transition, thus leading to

TABLE IV. Internal-conversion coefficients for the 177- and 153-keV transitions, for the K shell (α_K), the sum of the L and M shells (α_{L+M}), and the total (α_{total}). The second column gives the internal-conversion coefficients deduced in this work, as described in the text. The six right-most columns give the values for different multipolarities, as calculated by the code BRICC [31].

			177 keV	($M1$)			
	This work	$E1$	$M1$	$E2$	$M2$	$E3$	$M3$
α_K	2.1(13)	0.096	2.48	0.203	10.3	0.43	25.6
α_{L+M}	0.7(4)	0.024	0.570	0.671	4.57	10.4	38.4
α_{total}	2.8(20)	0.121	3.09	0.921	15.2	11.6	66.9
			153 keV	($E2$)			
	This work	$E1$	$M1$	$E2$	$M2$	$E3$	$M3$
α_K	<0.68	0.135	3.73	0.255	16.7	0.456	38.9
α_{L+M}	2.2(14)	0.034	0.860	1.27	8.09	22.6	80.8
α_{total}	2.2(14)	0.172	4.65	1.61	25.4	24.7	126

a final tentative assignment of $(7/2)^+$ for the 177-keV level. This is in agreement with the assignment of the analogous state in the isotone ^{215}Rn from Ref. [33], and is discussed in Sec. V. A tentative assignment of $(7/2)^+$ is also made for the 753-keV state, indicated by the low α-decay HF of 2.7 from the ^{221}Th $7/2^+$ ground state, and is also in line with the assignment for the analogous state in ^{215}Rn [33].

A comparison of the intensities of the 227- and 526-keV γ rays in coincidence with the 7735-keV α particle suggests an $E1$ character for the 227-keV transition. This would imply negative parity for the state at 227 keV with possible assignments $J^\pi = (7/2, 9/2, 11/2)^-$. An $11/2^-$ assignment for the state is ruled out as the 526-keV transition is inferred not to have an $M2$ multipolarity. This results from the observation of the 526-keV γ ray from the 753-keV state, despite competing with 576- and 753-keV transitions which are assigned as $M1$ transitions from the spins and parities already assigned. The 227-keV state is therefore tentatively assigned as $(7/2,9/2)^-$, differing from the tentative $(11/2)^-$ assignment of the analogous state in ^{215}Rn.

These spin and parity assignments would then suggest multipolarities for the 422- and 526-keV transitions of $E2$ and $E1$, respectively. The γ-ray intensities within cascades in coincidence with the 7735-keV α particle are all consistent with the multipolarity assignments.

V. DISCUSSION

A. ^{221}Th → ^{217}Ra α decays

The α decays of ^{221}Th identified in this work can be compared to those reported previously, as detailed in Table I. The α decays identified here with $E_\alpha = 7735$, 8148, and 8471 keV correspond to the previously reported α decays listed in the table. The energies of these transitions are reasonably consistent in all of the previous work, and in the work presented here. The α decay with $E_\alpha = 8247$ keV, observed here with a branching ratio of $b_\alpha = 1.51(12)\%$, was not reported in previous work. It is possible that this α decay corresponds to the α decay with $E_\alpha = 8265(10)$ keV ($b_\alpha = 4\%$) reported by Andreyev *et al.* [7], as their energies differ only by approximately 2σ. However, this is unlikely as there are significant differences between the energy and branching ratio for that decay compared with the α decay of $E_\alpha = 8247$ keV reported here, whereas the three main α decays reported in the same work [7] have energies and branching ratios with values very similar to those observed here. Therefore, in the present work the α decays with $E_\alpha = 7951(8)$ keV [$b_\alpha = 0.14(3)\%$] and $E_\alpha = 8247(3)$ keV [$b_\alpha = 1.51(12)\%$] can be considered new observations.

Regarding the α decay reported in Ref. [7] with α-particle energy 8375 keV, the possibility of (α+ce) summing should be considered. It may be expected that signals with this energy would arise from the summing of the 8148-keV α particles with K internal-conversion electrons from the subsequent 331-keV transition, which have $E_{ce} = 227$ keV. In the present data, DSSD signals with this energy were observed in coincidence with K x rays of radium with energies around 86 and 100 keV. As these coincident K x rays were present with the expected relative intensities, the counts at ≈8375 keV are assigned as resulting solely from conversion-electron summing. It is therefore assumed that the previously reported α decay with energy 8375 keV was incorrectly assigned.

B. Previous level schemes of ^{217}Ra

The level scheme of ^{217}Ra deduced here can be compared to those presented in earlier work. Level schemes of ^{217}Ra were constructed from in-beam γ-ray and conversion-electron spectroscopy experiments by Lönnroth *et al.* [11], Sugawara *et al.* [12], and Roy *et al.* [13]. The construction of these level schemes was guided by the results of the earlier ^{221}Th α-decay spectroscopy carried out by Valli *et al.* [5] and Torgerson *et al.* [6], in which two α decays to two excited states in ^{217}Ra were reported. In that work, the excitation energies of the states in ^{217}Ra were established from α-particle energies and, therefore, had large uncertainties of ≈10 keV. In the present work, $\alpha\gamma$-coincidence analysis has been used to establish the energies of the two excited states reported in Refs. [5,6] to be 330.7(2) and 752.6(2) keV, and three additional states have been firmly established at 177.0(2), 226.7(2), and 539.8(3) keV.

The level schemes derived in the work of Roy *et al.* [13] and Sugawara *et al.* [12] both include excited states with energies 331 and 540 keV, consistent with the present work. However, the level scheme from the work of Lönnroth *et al.* [11] contains transitions with energies of 330 and 539 keV but which do not populate the ground state. Both of the level schemes presented by Roy *et al.* [13] and Sugawara *et al.* [12] include transitions at 407 and 600 keV. The placement of the 407-keV transition by Sugawara *et al.*, from a $15/2^+$ state to the 221-keV $11/2^+$ state, defined the excitation energy of the $15/2^+$ state to be 737 keV. It was assumed in that work that the α decay with $E_\alpha = 7735$ keV would populate this state; however, in the present work the energy of the state populated by this decay has been established to be 753 keV. The level scheme derived in the present work is, therefore, in closest agreement with that presented by Roy *et al.* in Ref. [13].

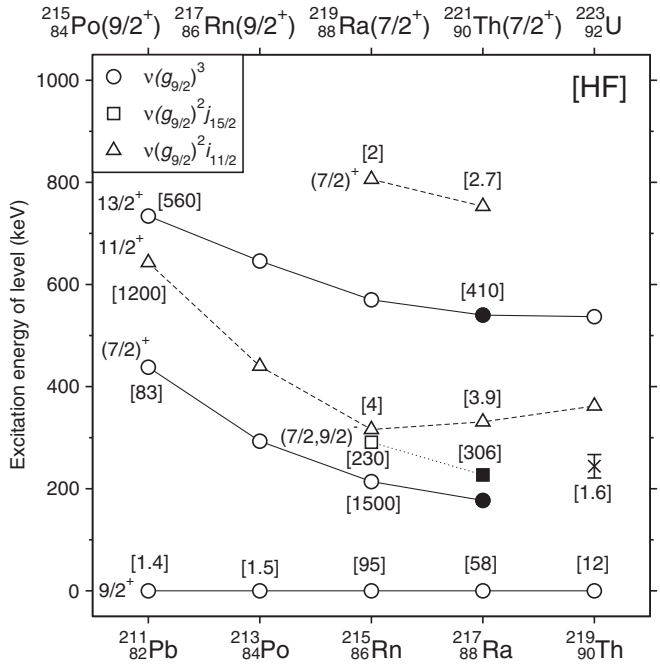

FIG. 8. Systematics of low-energy states in odd-A, $N = 129$ nuclei, above ^{208}Pb. The spins and parities of each set of states are shown and their spherical shell-model configurations are indicated by the symbols. Data are taken from Refs. [34–37] for ^{211}Pb, [38,39] for ^{213}Po, [33,40,41] for ^{215}Rn, [13,33] for ^{217}Ra, and [42,43] for ^{219}Th. Hindrance factors of α decays from parent nuclear states, indicated on the upper x axis, to the product states are shown in brackets from Refs. [33,35,43,44]. Solid symbols represent levels, or α decays to levels, that are newly observed. The state populated in ^{219}Th shown as a cross is taken from Ref. [43] and is discussed in the text.

C. Configurations of states

With $Z = 88$ and $N = 129$, the nucleus ^{217}Ra has three neutrons and six protons outside of the doubly magic ^{208}Pb core. The low-lying states of ^{217}Ra have previously been associated with configurations of the three valence neutrons [11–13,33] which can occupy spherical shell-model orbitals $g^+_{9/2}$, $i^+_{11/2}$, and $j^-_{15/2}$. Figure 8 shows the systematics of low-lying energy levels in the odd-A, $N = 129$ nuclei for $82 \leqslant Z \leqslant 90$. The solid symbols represent new levels, or α-decay HFs to levels, presently reported in ^{217}Ra. The energies, spins, parities, and spherical shell-model configuration assignments shown on the figure were taken from Refs. [34–37] (^{211}Pb), [38,39] (^{213}Po), [33,40,41] (^{215}Rn), [13,33] (^{217}Ra), and [42,43] (^{219}Th). The 291-keV state in ^{215}Rn identified in Ref. [33] was reassigned with $J^\pi = (7/2, 9/2)^-$ in light of the present results for ^{217}Ra. Also shown in square brackets are the known α-decay HFs to the levels taken from Refs. [33,35,43,44]. Single-particle configurations of the two new states observed in ^{217}Ra have been assigned based on their possible spins and parities (as described in Sec. IV C), regional energy systematics, and comparison of the branching ratios in the level schemes. The α-decay HFs to the states also helped to assign their properties. A clear similarity in the fine structures of the decays from ^{219}Ra and ^{221}Th is seen. This was previously noted in Ref. [33] where the α-decaying states in both of these nuclei were also assigned configurations from a model which describes orbitals in the presence of a permanent quadrupole-octupole deformed nuclear potential [4].

A comparison of the α-decay fine structure from odd-A, $N = 131$ isotones above ^{208}Pb, indicated on the upper x axis of Fig. 8, can help to shed light on the structure of these parent ground states. The $N = 131$, odd-A isotones $^{215}_{84}$Po, $^{217}_{86}$Rn, $^{219}_{88}$Ra, $^{221}_{90}$Th, and $^{223}_{92}$U have all been shown to decay by α-particle emission from their ground states [33,35,43,44]. The ground states of the five daughter nuclei, $^{211}_{82}$Pb, $^{213}_{84}$Po, $^{215}_{86}$Rn, $^{217}_{88}$Ra, and $^{219}_{90}$Th, have all been assigned to have $J^\pi = 9/2^+$, $\nu(g_{9/2})^3$ spherical shell configurations [13,33,36,39,42]. The nuclei $^{215}_{84}$Po and $^{217}_{86}$Rn have unhindered, and therefore dominant, α decays to the ground states of their daughter nuclei, $^{211}_{82}$Pb and $^{213}_{84}$Po. The unhindered α decay implies the same spherical shell-model configurations for the ground states of the parents. For the next two isotones, $^{219}_{88}$Ra and $^{221}_{90}$Th, the similarity of their α-decay fine structures to ^{215}Rn and ^{217}Ra, as discussed, implies the same ground-state configurations in both parent nuclei, which differ from that of the daughter nuclei. The ground states of both parent nuclei have been assigned with $J^\pi = 7/2^+$ [32,33], which are consistent with ground states described by the reflection-asymmetric model, noted in Ref. [45]. However, the possible reflection asymmetry of the ^{219}Ra and ^{221}Th ground states is still an open question [46,47].

Included also in Fig. 8 are recent results from the α-decay study of ^{223}U [43]. It is assumed that the higher-energy α decay populates the $9/2^+$ $\nu(g_{9/2})^3$ ground state of ^{219}Th. The excited state at 244(23) keV, populated by an unhindered α decay, is represented by a cross. It is proposed in Ref. [43] that this populated level is the $11/2^+$ $\nu(g_{9/2})^2 i_{11/2}$ state, as this was only assigned tentatively at 362 keV following a γ-ray study [42]. This leads to a $7/2^+$ $\nu(g_{9/2})^4 i_{11/2}$ assignment for the decaying ground state of ^{223}U, continuing the trend observed in the odd-A, $N = 131$ isotones ^{219}Ra and ^{221}Th which are consistent with asymmetric-deformation model predictions. However, a 244(23)-keV energy for the $11/2^+$ $\nu(g_{9/2})^2 i_{11/2}$ state would mark a clear departure in energy systematics from the states in ^{215}Rn and ^{217}Ra, which have been unambiguously and precisely identified with $\alpha\gamma$-coincidence analysis. Also, the HF of 1.6 to the state is significantly lower than the values of 4 and 3.9 to the analogous states in ^{215}Rn and ^{217}Ra. Considering the presently extended systematics of the $(7/2,9/2)^-$ $\nu(g_{9/2})^2 j_{15/2}$ states, the populated 244(23)-keV level in ^{219}Th appears to fit in well with these. This would lead to the assignment of the ^{223}U ground state to a $\nu(g_{9/2})^2 j_{15/2}$ configuration, which would be somewhat unexpected. Clearly an $\alpha\gamma$-coincidence study would be of great interest to better understand the α-decay fine structure of ^{223}U and the ^{219}Th level scheme populated.

VI. SUMMARY

Fine structure in the α decay of ^{221}Th has been studied using $\alpha\gamma$-coincidence measurements, in an experiment at the

Accelerator Laboratory of the University of Jyväskylä in Finland. The nucleus ^{221}Th was produced in the ^{208}Pb(^{18}O, $5n$) reaction. The recoiling ^{221}Th evaporation residues were separated from the primary beam using the RITU recoil separator, before being implanted into double-sided silicon strip detectors behind the focal plane. Decays of the implanted nuclei were detected using the DSSDs themselves and three Clover HPGe detectors surrounding the DSSDs. The α decay of ^{221}Th populated states in the daughter nucleus ^{217}Ra. Precise excitation-energy measurements of the states in ^{217}Ra have enabled the construction of a level scheme of its low-lying states. Two α-decay branches from ^{221}Th and two states in ^{217}Ra have been newly observed. The α-decay systematics of the odd-A, $N = 131$ isotones above ^{208}Pb were used to interpret the ground-state configurations of these nuclei, including the recent results from ^{223}U [43]. It was suggested that the excited state populated in ^{219}Th by an unhindered α decay may not be the $11/2^+$, $\nu(g_{9/2})^2 i_{11/2}$ configuration suggested in Ref. [43], implying also that the α-decaying ground state of ^{223}U is not the $7/2^+$ state with the same single-particle configuration. However, it was suggested that the α decay of this particular nucleus should be further examined.

ACKNOWLEDGMENTS

This work is supported in part by the following bodies: STFC (UK) under Grant Award No. ST/L005808/1 (UWS); the EU Seventh Framework Programme, Integrating Activities Transnational Access, Project No. 262010 (ENSAR); the Academy of Finland under the Finnish Centre of Excellence Programme (Nuclear and Accelerator Based Physics Programme at JYFL); the Scottish Universities Physics Alliance (SUPA); the Slovak Research and Development Agency under Contract No. APVV-15-0225; the Slovak grant agency VEGA (Contract No. 2/0129/17); and the project ITMS code 26210120023, supported by the Research and Development Operational Programme funded by ERDF (30%). The authors would also like to acknowledge GAMMAPOOL support for the JUROGAM HPGe detectors.

APPENDIX: ΔE FORMULA DERIVATION

First give the total energy recorded following an α decay from a nucleus implanted into a detector, E'_α, in terms of the α-particle energy, where the recoiling energy of the product nucleus is given as E_R:

$$E'_\alpha = E_\alpha + RE_R, \tag{A1}$$

and conservation of momentum between the recoiling nucleus and α particle, with masses M_R and M_α respectively, determines,

$$E_R = E_\alpha M_\alpha / M_R, \tag{A2}$$

which is substituted into Eq. (A1),

$$E'_\alpha = E_\alpha[1 + RM_\alpha/M_R]. \tag{A3}$$

Then find the difference between the two α-particle energies $E_{\alpha 1}$ and $E_{\alpha 2}$, where the total energy of an α decay is given as Q:

$$Q_{\alpha 2} = Q_{\alpha 1} - E_\gamma, \tag{A4}$$

$$E_{\alpha 2}[1 + M_\alpha/M_R] = E_{\alpha 1}[1 + M_\alpha/M_R] - E_\gamma, \tag{A5}$$

$$E_{\alpha 2} - E_{\alpha 1} = -\frac{E_\gamma}{1 + M_\alpha/M_R}. \tag{A6}$$

Find the difference in measured energy between the summed α_2 and conversion electron with that of the α_1,

$$\Delta E = (E'_{\alpha 2} + E_{ce}) - E'_{\alpha 1}, \tag{A7}$$

substitute in Eq. (A3),

$$\Delta E = [(E_{\alpha 2} - E_{\alpha 1})(1 + RM_\alpha/M_R)] + E_{ce}, \tag{A8}$$

then Eq. (A6) and $E_{ce} = E_\gamma - BE$,

$$\Delta E = E_\gamma \left[1 - \frac{1 + RM_\alpha/M_R}{1 + M_\alpha/M_R}\right] - BE. \tag{A9}$$

Finally, we can approximate $M_\alpha/M_R \simeq 4/(A-4)$ and substitute into Eq. (A9) to give

$$\Delta E \simeq E_\gamma \left[\frac{4}{A}(1 - R)\right] - BE. \tag{A10}$$

[1] I. Ahmad and P. A. Butler, Annu. Rev. Nucl. Part. Sci **43**, 71 (1993).
[2] P. A. Butler and W. Nazarewicz, Rev. Mod. Phys. **68**, 349 (1996).
[3] P. A. Butler, J. Phys. G: Nucl. Part. Phys. **43**, 073002 (2016).
[4] G. A. Leander and R. K. Sheline, Nucl. Phys. A **413**, 375 (1984).
[5] K. Valli, E. K. Hyde, and J. Borggreen, Phys. Rev. C **1**, 2115 (1970).
[6] D. F. Torgerson and R. D. Macfarlane, Nucl. Phys. A **149**, 641 (1970).
[7] A. N. Andreyev, D. D. Bogdanov, V. I. Chepigin, A. P. Kabachenko, S. Sharo, G. M. Ter-Akopian, and A. V. Yeremin, Z. Phys. A **337**, 229 (1990).
[8] F. P. Heßberger, S. Hofmann, D. Ackermann, V. Ninov, M. Leino, S. Saro, A. Andreyev, A. Lavrentev, A. G. Popeko *et al.*, Eur. Phys. J. A **8**, 521 (2000).
[9] P. Kuusiniemi, J. F. C. Cocks, K. Eskola, P. T. Greenlees, K. Helariutta, P. Jones, R. Julin, S. Juutinen, H. Kankaanpää, A. Keenan *et al.*, Acta Phys. Pol. B **32**, 1009 (2001).
[10] Z. Liu, J. Kurcewicz, P. J. Woods, C. Mazzocchi, F. Attallah, E. Badura, C. N. Davids, T. Davinson, J. Döring, H. Geissel

et al., Nucl. Instrum. Methods Phys. Res., Sect. A **543**, 591 (2005).
[11] T. Lönnroth, D. Horn, C. Baktash, C. J. Lister, and G. R. Young, Phys. Scr. **28**, 459 (1983).
[12] M. Sugawara, Y. Gono, and Y. Itoh, J. Phys. Soc. Jpn. **53**, 2956 (1984).
[13] N. Roy, D. J. Decman, H. Kluge, K. H. Maier, A. Maj, C. Mittag, J. Fernandez-Niello, H. Puchta, and F. Riess, Nucl. Phys. A **426**, 379 (1984).
[14] J. Pakarinen, P. Papadakis, J. Sorri, R.-D. Herzberg, P. T. Greenlees, P. A. Butler, P. J. Coleman-Smith, D. M. Cox, J. R. Cresswell, P. Jones *et al.*, Eur. Phys. J. A **50**, 53 (2014).
[15] M. Leino, Nucl. Instrum. Methods Phys. Res., Sect. B **126**, 320 (1997).
[16] J. Uusitalo, P. Jones, P. Greenlees, P. Rahkila, M. Leino, A. N. Andreyev, P. A. Butler, T. Enqvist, K. Eskola, T. Grahn *et al.*, Nucl. Instrum. Methods Phys. Res., Sect. B **204**, 638 (2003).
[17] R. D. Page, A. N. Andreyev, D. E. Appelbe, P. A. Butler, S. J. Freeman, P. T. Greenlees, R.-D. Herzberg, D. G. Jenkins, G. D. Jones, P. Jones *et al.*, Nucl. Instrum. Methods Phys. Res., Sect. B **204**, 634 (2003).
[18] P. Rahkila, Nucl. Instrum. Methods Phys. Res., Sect. A **595**, 637 (2008).
[19] I. H. Lazarus, D. E. Appelbe, P. A. Butler, P. J. Coleman-Smith, J. R. Cresswell, S. J. Freeman, R.-D. Herzberg, I. Hibbert, D. T. Joss, S. C. Letts *et al.*, IEEE Trans. Nucl. Sci. **48**, 567 (2001).
[20] S. Hofmann, G. Münzenberg, K. Valli, F. HeßbergerJ. R. H. Schneider, P. Armbruster, B. Thuma, and Y. Eyal, GSI Scientific Report No. GSI-82-1, 1982 (unpublished), p. 241.
[21] M. S. Basunia, Nucl. Data Sheets **108**, 633 (2007).
[22] J. Chen and F. G. Kondev, Nucl. Data Sheets **126**, 373 (2015).
[23] E. Parr, J. F. Smith, P. T. Greenlees, K. Auranen, P. A. Butler, R. Chapman, D. M. Cox, D. M. Cullen, L. P. Gaffney, T. Grahn *et al.*, Phys. Rev. C **100**, 044323 (2019).
[24] F. P. Heßberger, S. Hofmann, G. Münzenberg, K.-H. Schmidt, P. Armbruster, and R. Hingmann, Nucl. Instrum. Methods Phys. Res., Sect. A **274**, 522 (1989).
[25] Ch. Theisen, A. Lopez-Martens, ad Ch. Bonnelle, Nucl. Instrum. Methods Phys. Res., Sect. A **589**, 230 (2008).
[26] W. J. Huang and G. Audi, EPJ Web Conf. **146**, 10007 (2017).
[27] P. Hovington, D. Drouin, and R. Gauvin, Scanning **19**, 1 (1997).
[28] J. F. Ziegler, M. D. Ziegler, and J. P. Biersack, Nucl. Instrum. Methods Phys. Res., Sect. B **268**, 1818 (2010).
[29] M. O. Krause, J. Phys. Chem. Ref. Data **8**, 307 (1979).
[30] M. A. Preston, Phys. Rev. **71**, 865 (1947).
[31] T. Kibédi, T. W. Burrows, M. B. Trzhaskovskaya, P. M. Davidson, and C. W. Nestor, Nucl. Instrum. Methods Phys. Res., Sect. A **589**, 202 (2008).
[32] S. K. Tandel, M. Hemalatha, A. Y. Deo, S. B. Patel, R. Palit, T. Trivedi, J. Sethi, S. Saha, D. C. Biswas, and S. Mukhopadhyay, Phys. Rev. C **87**, 034319 (2013).
[33] R. K. Sheline, C. F. Liang, P. Paris, A. Gizon, and V. Barci, Phys. Rev. C **49**, 725 (1994).
[34] C. Ellegaard, P. D. Barnes, and E. R. Flynn, Nucl. Phys. A **259**, 435 (1976).
[35] C. F. Liang, P. Paris, and R. K. Sheline, Phys. Rev. C **58**, 3223 (1998).
[36] G. J. Lane, K. H. Maier, A. P. Byrne, G. D. Dracoulis, R. Broda, B. Fornal, M. P. Carpenter, R. M. Clark, M. Cromaz, R. V. F. Janssens *et al.*, Phys. Lett. B **606**, 34 (2005).
[37] A. I. Morales, G. Benzoni, A. Gottardo, J. J. Valiente-Dobón, N. Blasi, A. Bracco, F. Camera, F. C. L. Crespi, A. Corsi, S. Leoni *et al.*, Phys. Rev. C **89**, 014324 (2014).
[38] G. Ardisson, V. Barci, and O. El Samad, Phys. Rev. C **57**, 612 (1998).
[39] A. Astier and M.-G. Porquet, Phys. Rev. C **83**, 034302 (2011).
[40] A. M. Y. El-Lawindy, J. D. Burrows, P. A. Butler, J. R. Cresswell, V. Holliday, G. D. Jones, R. Tanner, R. Wadsworth, D. L. Watson, K. A. Connell *et al.*, J. Phys. G **13**, 93 (1987).
[41] M. E. Debray, M. Davidson, J. Davidson, A. J. Kreiner, M. A. Cardona, D. Hojman, D. R. Napoli, S. Lenzi, G. de Angelis, M. De Poli *et al.*, Phys. Rev. C **86**, 014326 (2012).
[42] W. Reviol, D. G. Sarantites, C. J. Chiara, M. Montero, R. V. F. Janssens, M. P. Carpenter, T. L. Khoo, T. Lauritsen, C. J. Lister, D. Seweryniak *et al.*, Phys. Rev. C **80**, 011304(R) (2009).
[43] M. D. Sun, Z. Liu, T. H. Huang, W. Q. Zhang, A. N. Andreyev, B. Ding, J. G. Wang, X. Y. Liu, H. Y. Lu, D. S. Hou *et al.*, Phys. Lett. B **800**, 135096 (2020).
[44] J. D. Bowman, R. E. Eppley, and E. K. Hyde, Phys. Rev. C **25**, 941 (1982).
[45] R. K. Sheline, Phys. Lett. B **197**, 500 (1987).
[46] L. A. Riley, P. D. Cottle, M. Fauerbach, V. S. Griffin, B. N. Guy, K. W. Kemper, G. S. Rajbaidya, and O. J. Tekyi-Mensah, Phys. Rev. C **62**, 021301(R) (2000).
[47] T. C. Hensley, P. D. Cottle, Vandana Tripathi, B. Abromeit, M. Anastasiou, L. T. Baby, J. S. Baron, D. Caussyn, R. Dungan, K. W. Kemper *et al.*, Phys. Rev. C **96**, 034325 (2017).